INSTITUTE OF PHYSICS PUBLISHING and INTERNATIONAL ATOMIC ENERGY AGENCY NUCLEAR FUSION
Nucl. Fusion **44** (2004) 869–875 PII: S0029-5515(04)81829-5

Enhanced Dα confinement mode: a theoretical model

André L. Rogister

Institut für Plasmaphysik, Forschungszentrum Jülich GmbH, EURATOM - FZJ Assoziation, Trilateral Euregio Cluster, D-52425 Jülich, Germany

E-mail: a.rogister@fz-juelich.de

Received 27 February 2003, accepted for publication 4 June 2004
Published 5 July 2004
Online at stacks.iop.org/NF/44/869
doi:10.1088/0029-5515/44/8/005

Abstract
It has been shown in a previous paper that the neoclassical theory of plasma rotation explains well the large toroidal velocity that is measured in the core of edge localized mode (ELM)-free ALCATOR C-Mod H-mode discharges. It has also been noted that the gradient of the toroidal/parallel velocity estimated at the pedestal inflexion point approaches the value required for the onset of the parallel velocity shear Kelvin–Helmholtz (PVS K–H) instability when the discharge is about to undergo an ELM-free to enhanced Dα (EDA) transition. The wavenumbers and frequencies of weakly unstable PVS K–H oscillations are consistent with those of the quasi-coherent mode that is observed in the EDA, but not in the ELM-free, regime—hence the suggestion, which is explored here further, that the transition is the consequence of PVS K–H instability onset. It is at first noted that the neoclassical expression for the toroidal velocity gradient warrants that large values of the safety factor, q, and of the triangularity parameter, δ, favour the transition, as observed. It is also shown that outward convection of toroidal momentum reduces the toroidal velocity gradient and, therefore, the instability growth rate. The anomalous particle flow and the particle confinement time in EDA discharges are then estimated on the assumption that anomalous transport maintains the velocity gradient at the threshold value. The power balance consideration shows that heat transport across the H-mode pedestal is neoclassical, at most. A simple expression of the ratio of particle and energy fluxes is then obtained; the ratio τ_P/τ_E of the respective confinement times is in the range of reported values (although it must be noted that it is difficult to quantify τ_P as it varies rapidly across the edge layer). The scenario assumes that the H-mode pedestal of EDA discharges (the unstable layer where anomalous transport occurs) is impermeable for neutrals since charged particles issuing from ionization would otherwise accumulate in the core; experimental parameters justify this assumption. The possibility of matching simultaneously the requirements for PVS K–H instability onset and non-permeability to neutrals in large devices is discussed.

PACS numbers: 52.25.Fi, 52.35.Kt, 52.35.Ra

1. Introduction

Neoclassical theory explains well the fast toroidal co-rotation (i.e. rotation in the direction of the plasma current) which is observed in the core of high collisionality ALCATOR C-Mod edge localized mode (ELM)-free H-mode discharges [1, 2] (those are obtained in the lower single null operation with either Ohmic or Ohmic and ion cyclotron wave (ICW) heating; there is therefore no momentum input). It also suggests that the velocity gradient is much larger across the temperature pedestal than in the core and increases rapidly with the safety factor, q.

The discharge discussed in [1] was characterized by a value of $q_{95} = 3.4$, and we estimated $\partial \vec{U}_{\varphi,\mathrm{i}}/\partial r \approx -5.8 \times 10^6\,\mathrm{s}^{-1}$ at the pedestal's inflexion point ($\vec{U}_\mathrm{i}$ is the ion bulk velocity, φ and θ are the toroidal and poloidal angles, q_{95} refers to the magnetic surface that encloses 95% of the toroidal magnetic flux). That is comparable with $c_\mathrm{s}\partial_r \ln N_\mathrm{i} \approx -7.4 \times 10^6\,\mathrm{s}^{-1}$, the ratio of the sound speed, $c_\mathrm{s} = \sqrt{T_\mathrm{e}/m_\mathrm{i}}$, to the density length-scale, $L_\mathrm{N} = (\partial_r \ln N_\mathrm{i})^{-1}$, implying that parallel velocity shear Kelvin–Helmholtz (PVS K–H) oscillations are about to get unstable (following [3, 4], the instability criterion is $|\partial_r U_{\|,\mathrm{i}}/\sqrt{2}c_\mathrm{s}\partial_r \ln N_\mathrm{i}|_\mathrm{thr} = 1$ if $T_\mathrm{i} = T_\mathrm{e}$, a condition likely to be met under the present conditions).

In ALCATOR C-Mod, a transition from ELM-free to enhanced Dα (EDA) behaviour occurs when q_{95} is in the range $3.5 < q_{95} < 4$ [5, 6]. EDA discharges are characterized by a low particle confinement time and the presence of a quasi-coherent (QC) oscillation with frequency $f \approx 120$ kHz and poloidal wave number $k_\theta \approx 400\,\mathrm{m}^{-1}$. Since similar frequency and wavenumber ranges are expected for weakly unstable PVS K–H oscillations, the transition was tentatively associated with the onset of the PVS K–H instability in section 7.3 of [1].

According to theory [3, 4], these weakly unstable PVS K–H oscillations propagate in the directions defined by $k_\parallel/k_\beta = \partial_r U_{\parallel,\mathrm{i}}/2\Omega_\mathrm{i} = a_\mathrm{s}|\partial_r \ln N_\mathrm{i}|\mathrm{sign}(\partial_r U_{\parallel,\mathrm{i}})/\sqrt{2}$, where $k_\parallel$ and k_β are the parallel and binormal components of the wave vector, sign $X = X/|X|$ and $a_\mathrm{s} = c_\mathrm{s}/\Omega_\mathrm{i}$ (Ω_i is the ion cyclotron frequency). Introducing $k_\beta \approx k_\theta = 400\,\mathrm{m}^{-1}$ yields $k_\parallel \approx 10\,\mathrm{m}^{-1}$ and $qRk_\parallel \approx 23$ (the major radius of ALCATOR C-Mod is $R = 0.67$ m); under those conditions, the modes are not tied to a particular rational surface, in further agreement with observations.

The QC oscillation appears to control efficiently the edge gradients through a continuous rather than an intermittent process. Being therefore characterized by the absence of large ELMs, reduced particle confinement and mere Ohmic or Ohmic and ICW heating, the EDA H-mode is particularly appropriate for reactor operation (here, α particle heating will replace ICW heating). The main purpose of this paper is to show that identification of the QC mode with a weakly (or marginally) unstable PVS K–H oscillation also explains the observed stationary reduction of particle confinement. The scenario assumes that the excited oscillation prevents any increase in the toroidal velocity gradient beyond the threshold value $\partial_r U_{\varphi,\mathrm{i}} = (\partial_r U_{\varphi,\mathrm{i}})_\mathrm{thr}$, a working hypothesis that will be discussed in a forthcoming paper on the quasi-linear theory of anomalous transport, and that the neutrals entering the plasma do not penetrate beyond the unstable layer (the pedestal width) that is characterized by large velocity gradients.

If $\partial_r U_{\varphi,\mathrm{i}} = (\partial_r U_{\varphi,\mathrm{i}})_\mathrm{thr}$, then the rate, $m_\mathrm{i}N_\mathrm{i}U_{r,\mathrm{i}}\partial_r U_{\varphi,\mathrm{i}}$, of radial convection of toroidal momentum, which is predicted by the toroidal momentum equation, yields the anomalous particle flux $\Gamma_\mathrm{an} = N_\mathrm{i}U_{r,\mathrm{i}}$. A simplified expression of the latter is (see section 3)

$$\Gamma_\mathrm{an} \approx 0.166\left(\frac{a_\mathrm{i,p}}{L_\mathrm{T}}\right) q^2\nu_\mathrm{i}a_\mathrm{i}^2\eta_\mathrm{i}\partial_r N_\mathrm{i} > 0, \qquad (1)$$

where $a_\mathrm{i} = c_\mathrm{i}/\Omega_\mathrm{i}$, $a_\mathrm{i,p} = |B_\varphi/B_\theta|a_\mathrm{i}$, $L_\mathrm{T} = (\partial_r \ln T_\mathrm{i})^{-1}$ and $\eta_\mathrm{i} = \partial_r \ln T_\mathrm{i}/\partial_r \ln N_\mathrm{i}$; ν_i is the ion collision frequency, following Braginskii [7]. The reason why Γ_an has to be positive, i.e. the ion and electron fluxes ($N_\mathrm{e}U_{r,\mathrm{e}} = N_\mathrm{i}U_{r,\mathrm{i}}$) are directed outwards, is discussed in section 3.

It has been shown in [1] that energy transport across the H-mode barrier is neoclassical, at most. The ratio of the energy and particle fluxes then takes on a relatively simple form (see section 4.4):

$$\frac{q_{r,\mathrm{i}}}{\Gamma_\mathrm{an}T_\mathrm{i}} \approx \frac{20(-L_\mathrm{T})}{a_{\mathrm{i},p}} \qquad (2)$$

from which the ratio, τ_P/τ_E, of the particle and energy confinement times can be estimated. The estimation falls in the range of reported values, but it must be noted that the quantification of τ_P is difficult as it varies rapidly across the pedestal.

The theory of plasma rotation is reviewed in section 2. The anomalous particle transport model is formulated in section 3. Its suitability (tests of marginal stability criterion and density requirement) and the theoretical predictions (scaling to larger devices, anomalous particle flux and confinement time) are discussed in section 4. The results are summarized in section 5, which also contains additional comments.

2. Theory of plasma rotation

The equation

$$\begin{aligned} &m_\mathrm{i}[\partial_\mathrm{t}(N_\mathrm{i}U_{\varphi,\mathrm{i}}) + \partial_r(N_\mathrm{i}U_{r,\mathrm{i}}U_{\varphi,\mathrm{i}})] \\ &\quad = m_\mathrm{i}N_\mathrm{i}[\nu_\mathrm{iz}U_{\varphi,0} - \nu_\mathrm{cx}(U_{\varphi,\mathrm{i}} - U_{\varphi,0})] \\ &\quad\quad +\partial_r\left[\eta_{2,\mathrm{i}}\left(\frac{\partial U_{\varphi,\mathrm{i}}}{\partial r} - \frac{0.107q^2}{1+Q^2/S^2}\frac{\partial \ln T_\mathrm{i}}{\partial r}\frac{B_\varphi}{B_\theta}U_{\theta,\mathrm{i}}\right)\right] \end{aligned} \qquad (3)$$

describes the evolution of *total* toroidal momentum in a high collisionality plasma. Here

(i) the terms on the left-hand side correspond to the inertia;
(ii) the first term on the right-hand side represents the momentum source associated with ionization of neutrals and the momentum sink associated with charge exchange; $\vec{U}_0$ is the neutral bulk velocity and ν_iz and ν_cx are their ionization and charge exchange rates;
(iii) the terms proportional to the classical viscosity coefficient $\eta_{2,\mathrm{i}} = 1.2N_\mathrm{i}T_\mathrm{i}\nu_\mathrm{i}/\Omega_\mathrm{i}^2$ arise from the toroidal component of the divergence of the stress tensor [8]; we note that the off-diagonal contribution that is proportional to the poloidal velocity, $U_{\theta,\mathrm{i}}$, is the only driving term in the absence of momentum injection (interestingly, an analysis of JFT-2M discharges with balanced injection [9] suggests the existence of such an off-diagonal component);
(iv) the dimensionless ratio Q/S is defined by $Q/S \equiv 0.51\Lambda[(eB_\varphi/\partial_r T_\mathrm{i})U_{\theta,\mathrm{i}} - 0.625(1+2\eta_\mathrm{i}^{-1})]$, where $\Lambda \equiv \hat{\nu}_\mathrm{i}(a_\mathrm{i})_\mathrm{p}/L_\mathrm{T}$, $\hat{\nu}_\mathrm{i} = qR\nu_\mathrm{i}/c_\mathrm{i}$ is the appropriate collisionality parameter and $(a_\mathrm{i})_\mathrm{p}/L_\mathrm{T}$ the ratio of the ion 'poloidal gyro-radius' to the temperature length-scale; we note that the factor $[1+Q^2/S^2]^{-1}$ also appears in the expression of the ion heat flux, leading to *sub-neoclassical* energy transport [10]; we estimated $(\hat{\nu}_\mathrm{i})_\mathrm{inf} \cong 1.57$ and $[1+Q^2/S^2]_\mathrm{inf}^{-1} \cong 0.56$ at the pedestal inflexion point, $r = r_\mathrm{inf}$, of the discharge analysed in [1] (reference discharge); the high collisionality description applies when $\hat{\nu}_\mathrm{i} > 0.222$ [11].

If we neglect, for simplicity (see appendix), the first term on the right-hand side of equation (3), straightforward integration yields, under stationary conditions,

$$(\partial_r - D_\mathrm{i}^{-1}U_{r,\mathrm{i}})U_{\varphi,\mathrm{i}} = L^{-1}U_{\theta,\mathrm{i}}, \qquad (4)$$

where $D_\mathrm{i} = \eta_{2,\mathrm{i}}/m_\mathrm{i}N_\mathrm{i} = 1.2\nu_\mathrm{i}a_\mathrm{i}^2$ and

$$L^{-1} \equiv 0.107q^2\left(1+\frac{Q^2}{S^2}\right)^{-1}\left(\frac{B_\varphi}{B_\theta}\right)\partial_r \ln T_\mathrm{i} \qquad (5)$$

(the integration constant vanishes as $U_{r,\mathrm{i}} \to 0$ and $\partial_r \to 0$ in the plasma core).

Below the instability threshold, the radial flow velocity is small and the inertia term can be neglected. Equation (4) then yields

$$U_{\varphi,\mathrm{i}} = \int_{r_\mathrm{s}}^{r} L^{-1}U_{\theta,\mathrm{i}}\,\mathrm{d}r', \qquad (6)$$

where r_s is the effective radius of the last closed magnetic surface (LCMS; r_s can be specified, knowing the position of the magnetic separatrix and the shape of the cross section); we have assumed, in the absence of any contrary evidence, that

$U_{\varphi,\mathrm{i}}(r_\mathrm{s}) = 0$ without external momentum input. The poloidal velocity can be approximated by

$$U_{\theta,\mathrm{i}} = \frac{\kappa \partial_r T_\mathrm{i}}{e_\mathrm{i} B_\varphi} = \kappa \left(\frac{B}{B_\varphi}\right) a_\mathrm{i} c_\mathrm{i} \partial_r \ln T_\mathrm{i}, \qquad (7)$$

where $\kappa = -1.83$ in the high collisionality regime [8, 12]. Equation (7) is not exact if either Λ is finite, see [8], or the ratio $U_{\varphi,\mathrm{i}}/c_\mathrm{s}$ is finite, see [12]; it is used here for simplification purposes. A slightly different value of $\kappa(= -2.1)$ is given by Hazeltine [13]; see [12] for further comments. The integrand in equation (6) is thus proportional to $(\partial_r T_\mathrm{i})^2/T_\mathrm{i}$, leading to a large variation in $U_{\varphi,\mathrm{i}}(r)$ across the H-mode pedestal and a smaller one across the entire core. Equation (6) yields the correct estimate for the large toroidal co-rotation ($U_{\varphi,\mathrm{i}} \cong +35\,\mathrm{km\,s^{-1}}$) that is measured on the magnetic axis of ELM-free H-mode discharges [1] (L^{-1} being negative and $U_{\theta,\mathrm{i}}$ positive (since $\partial_r T_\mathrm{i} < 0$; B_φ and B_θ are positive by convention), the toroidal velocity is positive, i.e. in the direction of the plasma current ($B_\theta > 0$ implies $J_\varphi > 0$)). There is unfortunately no direct experimental information on the toroidal velocity in the pedestal.

3. Parallel velocity shear instability and anomalous particle transport

A plasma is PVS K–H unstable if the gradient in a direction orthogonal to $\vec{B}$ of the parallel component of the ion streaming velocity exceeds a threshold value given by

$$|\partial_r U_{\|,\mathrm{i}}|_\mathrm{thr} = \sqrt{2} c_\mathrm{i} |\alpha \partial_r \ln N_\mathrm{i}|; \qquad (8)$$

here, following [3, 4], $\alpha(r) = 1$ if $T_\mathrm{i} = T_\mathrm{e}$. In a tokamak, $B_\theta U_{\theta,\mathrm{i}} \ll B_\varphi U_{\varphi,\mathrm{i}}$, so that $U_{\|,\mathrm{i}}$ may be identified with $B_\varphi U_{\varphi,\mathrm{i}}/B$. As observed in section 2, the relations $U_{r,\mathrm{i}} = 0$ and $\partial_r U_{\varphi,\mathrm{i}} = L^{-1} U_{\theta,\mathrm{i}} < 0$ apply if the plasma is stable, i.e. if $-L^{-1}U_{\theta,\mathrm{i}} + \sqrt{2} c_\mathrm{i} \alpha \partial_r \ln N_\mathrm{i} < 0$ (in view of (8) and $U_{\|,\mathrm{i}} = B_\varphi U_{\varphi,\mathrm{i}}/B$). Conversely, instability occurs, leading to $N_\mathrm{i} U_{r,\mathrm{i}} \neq 0$ if

$$-L^{-1}U_{\theta,\mathrm{i}} + \sqrt{2} c_\mathrm{i} \alpha \partial_r \ln N_\mathrm{i} > 0. \qquad (9)$$

The main assumption of this work is that anomalous transport freezes the toroidal velocity profile, $U_{\varphi,\mathrm{i}}(r)$, to the marginally unstable one, so that

$$\partial_r U_{\varphi,\mathrm{i}} = \sqrt{2} c_\mathrm{i} \alpha \partial_r \ln N_\mathrm{i} < 0, \qquad (10a)$$

(see equation (8)) when inequality (9) is fulfilled (while $-L^{-1}U_{\theta,\mathrm{i}}$ may exceed significantly its threshold value, $-\sqrt{2} c_\mathrm{i} \alpha \partial_r \ln N_\mathrm{i}$). Equations (10$a$) and (4) lead to

$$U_{\varphi,\mathrm{i}}(r) = \int_{r_\mathrm{s}}^{r} \sqrt{2} c_\mathrm{i} \alpha \partial_r \ln N_\mathrm{i} \, \mathrm{d}r' > 0 \qquad (10b)$$

(with $U_{\varphi,\mathrm{i}}(r_\mathrm{s}) = 0$) and

$$N_\mathrm{i} U_{r,\mathrm{i}} = \frac{D_\mathrm{i} N_\mathrm{i} [-L^{-1}U_{\theta,\mathrm{i}} + \sqrt{2} c_\mathrm{i} \alpha \partial_r \ln N_\mathrm{i}]}{U_{\varphi,\mathrm{i}}(r)} > 0. \qquad (11a)$$

The radial particle flux required to maintain the PVS K–H instability near the threshold is thus positive, i.e. directed outwards. That can be simply explained by noting that the contribution $m_\mathrm{i} U_{\varphi,\mathrm{i}} \partial_r (N_\mathrm{i} U_{r,\mathrm{i}})$, which appears on the left-hand side of equation (3), is equivalent to $m_\mathrm{i} \nu_\mathrm{iz} N_\mathrm{i} U_{\varphi,\mathrm{i}}$ in view of the continuity equation, $\partial_r (N_\mathrm{i} U_{r,\mathrm{i}}) = \nu_\mathrm{iz} N_\mathrm{i}$. Since the latter leads to $U_{r,\mathrm{i}} > 0$ in the pedestal if $U_{r,\mathrm{i}} \to 0$ in the core, it is straightforward to conclude that an outward particle flux slows down the toroidal rotation. As $|\partial_r U_{\varphi,\mathrm{i}}|$ is also reduced, the PVS K–H instability growth rate then decreases.

Equation (11a) can be rewritten as

$$N_\mathrm{i} U_{r,\mathrm{i}} = D_\mathrm{i} N_\mathrm{i} \frac{-L^{-1}U_{\theta,\mathrm{i}} + \sqrt{2} c_\mathrm{i} \alpha \partial_r \ln N_\mathrm{i}}{\sqrt{2}\alpha [c_\mathrm{i}(r) - c_\mathrm{i}(r_\mathrm{s})]} \qquad (11b)$$

if, for simplicity, α is constant and $\eta_\mathrm{i} = 2$ (hence $N_\mathrm{i}(r) \propto \sqrt{T_\mathrm{i}(r)}$ and $c_\mathrm{i} \partial_r \ln N_\mathrm{i} = \partial_r c_\mathrm{i}$). Using equations (5) and (7) as well as the functional dependence of D_i, equation (11b) yields the simple estimate

$$N_\mathrm{i} U_{r,\mathrm{i}} = 0.166 q^2 \nu_\mathrm{i} a_{\mathrm{i,p}} \left(\frac{a_\mathrm{i}}{L_\mathrm{T}}\right)^2 \frac{N_\mathrm{i}}{\alpha(1 + Q^2/S^2)} \qquad (11c)$$

if $c_\mathrm{i}(r)$ is significantly larger than $c_\mathrm{i}(r_\mathrm{s})$ and $-L^{-1}U_{\theta,\mathrm{i}}$ is significantly larger than $-\sqrt{2} c_\mathrm{i} \alpha \partial_r \ln N_\mathrm{i}$. Equation (1) is identical to (11c) if $\alpha(1 + Q^2/S^2) \cong 1$.

The product $|L^{-1}U_{\theta,\mathrm{i}}| \propto (\partial_r T_\mathrm{i})^2/T_\mathrm{i}$ decreases faster than $|\partial_r N_\mathrm{i}|$ going inwards from the pedestal inflexion point. As a result, the instability requirement (9) is violated for $r \leqslant r_0 < r_\mathrm{inf}$. In that region, the equations $\partial_r U_{\varphi,\mathrm{i}} = L^{-1}U_{\theta,\mathrm{i}}$ and $N_\mathrm{i} U_{r,\mathrm{i}} = 0$ apply in lieu of (10a) and (11a) (we note that the right-hand side of (11a) vanishes at $r = r_0$).

It has been shown earlier that magnetic shear plays no stabilizing role if, as is the case in the H-mode pedestal, $|L_\mathrm{N}| \ll |L_\mathrm{S}|$ ($L_\mathrm{S} = B_\varphi / B_\theta \partial_r \ln q$ is the magnetic shear length) [4]. Moreover, the marginally unstable modes are characterized by the relation

$$\frac{k_\|}{k_\beta} = \frac{\partial_r U_{\|,\mathrm{i}}}{2\Omega_\mathrm{i}} = \frac{a_\mathrm{i} |\partial_r \ln N_\mathrm{i}| \mathrm{sign}(\partial_r U_{\|,\mathrm{i}})}{\sqrt{2}} \qquad (12)$$

[3, 4]. We estimate that $k_\| q R \gg 1$ for the QC mode observed in ALCATOR C-Mod EDA discharges. Finite values of $k_\|$ are essential in explaining anomalous transport of parallel/toroidal momentum in the framework of quasi-linear theory (in preparation).

4. Theoretical predictions and comparison with experiment

We consider now the implications of the theory, compare them with experimental results from ALCATOR C-Mod and discuss the possibility of obtaining the EDA H-mode in larger devices.

4.1. *Marginal stability criterion*

Since the shot discussed in [1, 2] was close to the ELM-free to EDA transition, the marginal instability condition

$$\frac{L^{-1}U_{\theta,\mathrm{i}}}{\sqrt{2} c_\mathrm{i} \alpha \partial_r \ln N_\mathrm{i}} \equiv -\frac{0.14 q^2 \eta_\mathrm{i} a_{\mathrm{i,p}}}{L_\mathrm{T} \alpha (1 + Q^2/S^2)} \approx 1 \qquad (13)$$

should approximately be fulfilled at the pedestal inflexion point. Introducing the experimental parameters $q = 3.4$,

$\eta_i = 1.6$, $(L_T)_{inf} = -0.76\times10^{-2}$ m, $(a_{i,p})_{inf} = 0.29\times10^{-2}$ m and $(1 + Q^2/S^2)_{inf} = 1.77$, see [1], the value of the left-hand side is indeed $\approx 0.56/\alpha$. (We assume $N_i \cong N_e$ and, owing to the high density, $T_i \cong T_e$. The electron temperature profile is obtained with high spatial resolution using an edge Thomson scattering system (spatial resolution of 10^{-3} m) and cyclotron emission; the density profile is obtained using edge Thomson scattering and the visible continuum using a high spatial resolution (1.5×10^{-3} m) imaging CCD system).

Equation (13) shows that the PVS K–H instability threshold will be reached most easily if

(i) the safety factor, q, is sufficiently large: we recall that this is the major experimental requirement for the QC oscillation and the transition from ELM-free to EDA behaviour to occur;
(ii) L_N is sufficiently large (we recall that $\eta_i = L_N/L_T$), reflecting the fact that large values of $\partial_r \ln N_i$ stabilize the mode;
(iii) L_T is sufficiently small, reflecting the fact that the instability drive is proportional to $\partial_r U_{\varphi,i} \propto (\partial_r T_i)^2/T_i$; increasing the cross section triangularity, δ, leads experimentally to larger temperature gradients; it should thus also favour access to the EDA regime, as observed;
(iv) $c_i/B_\theta \propto c_i r_s/I$ is sufficiently large (I is the plasma current).

These considerations show that the QC mode with frequency $f \approx 120$ kHz and poloidal wavenumber $k_\theta \approx 400\,\mathrm{m}^{-1}$ that sets in at the ELM-free to EDA transition is probably excited by the PVS K–H instability. The product $k_\theta(a_i)_{inf} \approx 0.14$ is in the expected range. Correspondingly, $k_\theta(a_{i,p})_{inf} \approx 1.16$ and, in view of (12), $qRk_\parallel \approx 23$. Rational magnetic surfaces play no significant role if $qRk_\parallel \gg 1$, in further agreement with observations.

4.2. Density requirement and various profiles

The enhanced outward flux of ionized particles associated with the PVS K–H excited mode can lead to a stationary density profile only if ionization of neutrals mainly occurs within the unstable layer. We consider the neutrals as a fluid that may be described by the continuity and radial momentum equations,

$$\partial_r(N_0 U_{r,0}) = -\langle\sigma v\rangle_{iz} N_i N_0,$$

$$\partial_r[N_0(T_0 + m_0 U_{r,0}^2)] = -m_0(\langle\sigma v\rangle_{iz} + \langle\sigma v\rangle_{cx}) N_i N_0 U_{r,0}.$$

Here, N_0, T_0 and $U_{r,0}$ are the neutral density, temperature and radial bulk velocity; $\langle\sigma v\rangle_{iz}$ and $\langle\sigma v\rangle_{cx}$ are the ionization and charge exchange rate coefficients ($\nu_{iz} = \langle\sigma v\rangle_{iz} N_0$ and $\nu_{cx} = \langle\sigma v\rangle_{cx} N_0$). We shall neglect, for simplicity, but without proper justification, the variation of the temperature, T_0, and of the velocity, $U_{r,0}$, compared with that of the density, N_0. The above equations then have the solution

$$N_0(r) = N_0(r_{inf}) \exp \int_{r_{inf}}^{r} N_i \sqrt{\frac{m_0 \langle\sigma v\rangle_{iz}\langle\sigma v\rangle_{cx}}{T_0}}\,dr', \qquad (14a)$$

$$U_{r,0} = -\sqrt{\frac{T_0\langle\sigma v\rangle_{iz}}{m_0\langle\sigma v\rangle_{cx}}}, \qquad (14b)$$

($\langle\sigma v\rangle_{iz}$ and $\langle\sigma v\rangle_{cx}$ varying slowly indeed, $|\partial_r \ln U_{r,0}| \ll |\partial_r \ln N_0|$ would follow from $|\partial_r \ln T_0| \ll |\partial_r \ln N_0|$). Assuming $\eta_i = 2$ as before, $m_0 = m_i$ and $T_0 = T_i$ (which would be justified for $\langle\sigma v\rangle_{iz}/\langle\sigma v\rangle_{cx} \ll 1$), equation (14$a$) yields

$$N_0(r) = N_0(r_{inf}) \exp\left[\frac{r - r_{inf}}{\lambda_0}\right], \qquad (14c)$$

where

$$\lambda_0 = \frac{c_i(r)}{N_i(r)\sqrt{\langle\sigma v\rangle_{iz}\langle\sigma v\rangle_{cx}}} \qquad (15)$$

is (about) constant. The neutral and ionized particle fluxes are

$$\Gamma_i(r) = N_i U_{r,i} = -\Gamma_0(r) = -N_0 U_{r,0} = N_0 c_i \sqrt{\frac{\langle\sigma v\rangle_{iz}}{\langle\sigma v\rangle_{cx}}}. \qquad (16a)$$

(We note for completeness that the problem of neutral penetration has been solved exactly in [14] for $\nu_{cx}/\nu_{iz} \gg 1$ and $|\Lambda| \ll 1$; within a numerical factor, the parameter δ_i/Δ_i that occurs there is identical to Λ.)

In the temperature range of interest, $\langle\sigma v\rangle_{iz} = 3.3 \times 10^{-14}\,\mathrm{m^3\,s^{-1}}$ and $\langle\sigma v\rangle_{cx} = 3\langle\sigma v\rangle_{iz}/2$ [15]. Introducing $(N_i)_{inf} \approx 1.87 \times 10^{20}\,\mathrm{m^{-3}}$ and $(T_i)_{inf} = 165$ eV, (15) yields $\lambda_0 \approx 1.20 \times 10^{-2}$ m for the transition discharge [1]. This value of λ_0 is the same as that of the density length-scale at the pedestal inflexion point, $|L_N(r_{inf})| \cong 1.2 \times 10^{-2}$ m, implying that the edge is indeed impermeable for neutrals, as assumed. Comparing now equations (11c) and (16a) yields (with $(a_i)_{inf} = 0.035 \times 10^{-2}$ m, $(\nu_i)_{inf} = 0.6 \times 10^5\,\mathrm{s^{-1}}$ and the values quoted below, equation (13))

$$\left(\frac{N_0}{N_i}\right)_{inf} = 0.166 q^2 \frac{\nu_i}{\Omega_i} \frac{a_i (a_i)_p}{L_T^2} \sqrt{\frac{\langle\sigma v\rangle_{cx}}{\langle\sigma v\rangle_{iz}}} \frac{1}{\alpha(1 + Q^2/S^2)} = 0.54\alpha^{-1} \times 10^{-5}$$

and

$$\Gamma_i(r_{inf}) = \left(\frac{0.75}{\alpha}\right) \times 10^{20}\,\mathrm{m^{-2}\,s^{-1}}.$$

For a given temperature profile $T_i(r) = T_0(r)$, the ion and neutral density profiles can be obtained self-consistently from $N_i U_{r,i} = -N_0 U_{r,0}$ along with the fluid equations of the neutrals and equation (11a). For simplicity, we take, as in [1], a pedestal temperature profile of the form

$$T_i(r) = T_i(r_{inf})\left[1 - \tanh\frac{r - r_{inf}}{|L_T(r_{inf})|}\right] \qquad (17)$$

and assume, consistently with $\eta_i = 2$,

$$N_i(r) = N_i(r_{inf})\sqrt{1 - \tanh\frac{r - r_{inf}}{|L_T(r_{inf})|}}. \qquad (17')$$

We then obtain

$$\Gamma_i(r) = -\Gamma_0(r) = 0.75\alpha^{-1} \times 10^{20} \exp\left[\frac{r - r_{inf}}{\lambda_0}\right] \times\sqrt{1 - \frac{\tanh(r - r_{inf})}{|L_T(r_{inf})|}}\,\mathrm{m^{-2}\,s^{-1}}. \qquad (16b)$$

On physical grounds, $\partial_r \Gamma_i > 0$ holds. This imposes the constraint

$$\exp\left[-2\frac{r_s - r_{inf}}{|L_T(r_{inf})|}\right] \geqslant \frac{\lambda_0}{|L_T(r_{inf})|} - 1. \qquad (16c)$$

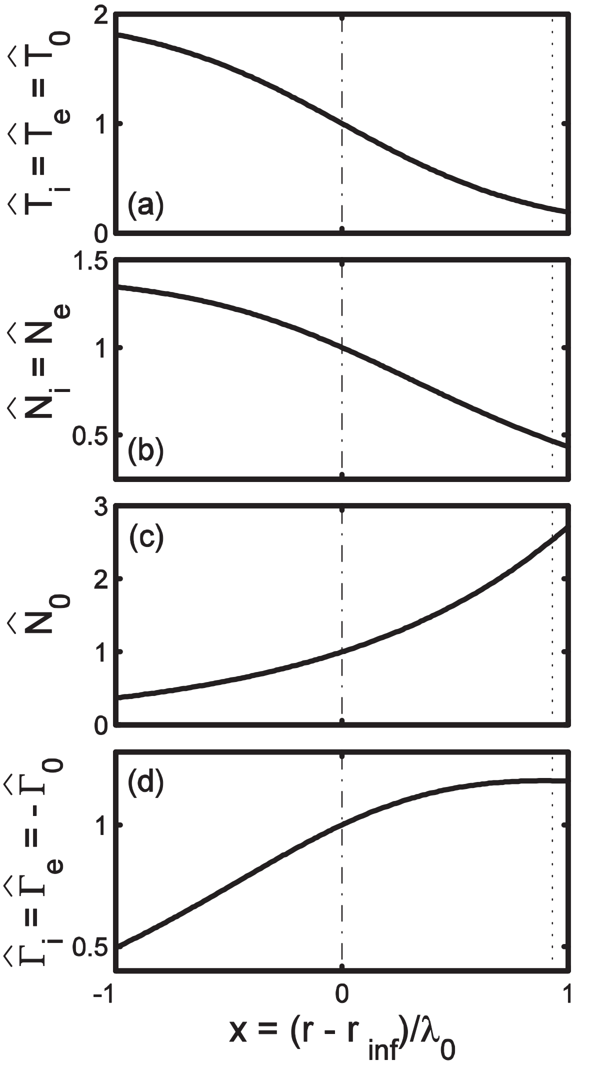

Figure 1. (*a*) Model temperature profile, $\hat{T}_{\rm i}(x) = \hat{T}_{\rm e}(x) = \hat{T}_0(x)$, equation (17); (*b*) model density profile, $\hat{N}_{\rm i}(x) = \hat{N}_{\rm e}(x)$, equation (17′); (*c*) neutral density profile, $\hat{N}_0(x)$, equation (14*c*); (*d*) particle fluxes, $\hat{\Gamma}_{\rm i}(x) = \hat{\Gamma}_{\rm e}(x) = -\hat{\Gamma}_0(x)$, equation (16*b*). $\hat{F}(x)$ is an abbreviation for $F[(r - r_{\rm inf})/\lambda_0]/F(0)$. We have assumed $|L_{\rm T}(r_{\rm inf})| = 0.76 \times 10^{-2}$ m and $\lambda_0 = 0.86 \times 10^{-2}$ m; the dotted line corresponds to $(r_{\rm s} - r_{\rm inf}) = 0.80 \times 10^{-2}$ m.

Introducing $|L_{\rm T}| \cong 0.76 \times 10^{-2}$ m and $\lambda_0 = 1.20 \times 10^{-2}$ m, (16*c*) leads to the condition $(r_{\rm s} - r_{\rm inf}) \leqslant 0.21 \times 10^{-2}$ m. This value depends both on the assumed density and temperature functionals and on the values of λ_0 and $|L_{\rm T}(r_{\rm inf})|$. It increases, for example, to $(r_{\rm s} - r_{\rm inf}) \leqslant 0.80 \times 10^{-2}$ m if $|L_{\rm T}(r_{\rm inf})| = 1 \times 10^{-2}$ m and $\lambda_0 = 1.20 \times 10^{-2}$ m or if $|L_{\rm T}| \cong 0.76 \times 10^{-2}$ m and $\lambda_0 = 0.86 \times 10^{-2}$ m. Figures 1(*a*)–(*d*) show the temperature, ion density, neutral density and particle flux profiles assuming $|L_{\rm T}| \cong 0.76 \times 10^{-2}$ m, $\lambda_0 = 0.86 \times 10^{-2}$ m and $(r_{\rm s} - r_{\rm inf}) = 0.80 \times 10^{-2}$ m.

It is clear that the above results are merely indicative for they rely on a number of working hypotheses. For clarity, we note also that the dimensions that have been quoted here refer to equivalent circular cross sections with radii $r = \sqrt{\kappa} r_{\rm equa}$, where κ (= 1.62) is the elongation of the cross section and $r_{\rm equa}$ the radius in the equatorial plane.

4.3. Scaling to larger devices

The large magnetic field of ALCATOR C-Mod allows working at high plasma densities and small neutral penetration depths. To discuss the requirements for achieving the EDA H-mode in larger devices, we shall

(a) assume identical temperature and density profiles,
(b) require the ratios $\lambda_0/|L_{\rm N}|$ and $q^2\eta_{\rm i} a_{\rm i,p}/L_{\rm T}$ (PVS K–H marginal instability requirement, equation (13)) to be invariant and
(c) require that the ratio of the line average density to the density limit $N_{\rm G} \propto B/qR$ (Greenwald, [16]) remain unchanged.

We obtain successively $|L_{\rm N}| \propto \lambda_0 \propto c_{\rm i}/N_{\rm i}\sqrt{\langle\sigma v\rangle_{\rm iz}\langle\sigma v\rangle_{\rm cx}} \propto qRT^{1/2}/B\sqrt{A_{\rm i}\langle\sigma v\rangle_{\rm iz}\langle\sigma v\rangle_{\rm cx}}$ (equation (15)) and $L_{\rm N} \propto q^3 R\eta_{\rm i}^2 T^{1/2} A_{\rm i}^{1/2}/r_{\rm s}B$ (equation (13)), where $A_{\rm i}$ is the ion atomic mass. Identifying the two expressions of $L_{\rm N}$ yields the condition

$$q^2\eta_{\rm i}^2 \propto \frac{r_{\rm s}}{A_{\rm i}\sqrt{\langle\sigma v\rangle_{\rm iz}\langle\sigma v\rangle_{\rm cx}}}. \tag{18}$$

Equation (18) suggests that the EDA H-mode could be obtained in larger devices either by working at higher values of q or by increasing $\eta_{\rm i}$ at the edge. The plasma will however ultimately enter the plateau and the banana regimes, in which case modified neoclassical equations are required. We also note that $\langle\sigma v\rangle_{\rm cx}$ increases by a factor ≈2 and $\langle\sigma v\rangle_{\rm iz}$ by ≈0.75 in the temperature range $T_0 \cong T_{\rm i} \in [10^2 - 10^3]$ eV.

4.4. Particle and energy confinement in EDA

Experiment suggests that energy transport is little affected at the transition from ELM-free to EDA behaviour. We have shown in [1] that the sub-neoclassical heat flux [10],

$$q_{{\rm i},r} = -\left[1 + 1.6q^2\left(1 + \frac{Q^2}{S^2}\right)^{-1}\right]\chi_{\perp,{\rm i}} N_{\rm i}\partial_r T_{\rm i}, \tag{19}$$

estimated at the pedestal inflexion point accounts for about half of the input power ($\chi_{\perp,{\rm i}} = 2a_{\rm i}^2\nu_{\rm i}$ is the classical ion heat conduction coefficient [7]); taking radiation losses into account leaves little room for anomalous energy transport. It is therefore relevant to compare (19) and the anomalous particle flux estimate (11*c*); that yields

$$\frac{q_{r,{\rm i}}}{N_{\rm i}U_{r,{\rm i}}} = 19\alpha\left(-\frac{L_{\rm T}}{a_{\rm i,p}}\right)T_{\rm i}. \tag{20}$$

The ratio of the particle and energy confinement times can be estimated easily, assuming the profiles $T_{\rm i} \propto [1 - (r/r_{\rm s})^2]$ and $N_{\rm i} \propto \sqrt{T_{\rm i}}$ throughout the entire discharge; we obtain

$$\frac{\tau_{\rm P}}{\tau_E} = \frac{\int {\rm d}V N_{\rm i}}{\int {\rm d}S N_{\rm i} U_{r,{\rm i}}}\frac{\int {\rm d}S(q_{r,{\rm i}} + q_{r,{\rm e}} + q_{\rm rad})}{\int {\rm d}V (3/2)(N_{\rm i}T_{\rm i} + N_{\rm e}T_{\rm e})}$$
$$\approx \frac{10(q_{r,{\rm i}} + q_{r,{\rm e}} + q_{\rm rad})_{\rm LCMS}}{9(N_{\rm i}U_{r,{\rm i}})_{\rm LCMS}(T_{\rm i} + T_{\rm e})_{\rm axis}}. \tag{21}$$

Since the heat flux $(q_{r,{\rm i}} + q_{r,{\rm e}} + q_{\rm rad})$ is constant through the pedestal and, at the inflexion point, $q_{r,{\rm i}}$ accounts for about half of the input power, we let $(q_{r,{\rm i}} + q_{r,{\rm e}} + q_{\rm rad})_{\rm edge} = 2(q_{r,{\rm i}})_{\rm inf}$.

Equation (21) thus yields, noting that $T_i = T_e$ and $T_{inf}/T_{axis} = 165/1200$ [1, 2],

$$\frac{\tau_P}{\tau_E} \sim \frac{7.5\alpha\Gamma_i(r_{inf})}{\Gamma_i(r_s)}. \qquad (21')$$

Introducing $(r_s - r_{inf}) = 0.80 \times 10^{-2}$ m, $|L_T(r_{inf})| = 0.76 \times 10^{-2}$ m and $\lambda_0 = 0.86 \times 10^{-2}$ m (see the discussion below equation (16*c*)) yields $\Gamma_i(r_{inf})/\Gamma_i(r_s) = 0.83$, so that $\tau_P/\tau_E \sim 6.2\alpha$. The reported values range from 3 to 4 [5, 6].

We note that figure 1(*d*), equation (16*b*) and the above considerations show the difficulty in quantifying a particle confinement time if λ_0 is comparable with L_N and L_T, as is the case when the edge is impermeable for neutrals (it actually depends on the influx of neutrals through the LCMS and the reference surface used).

5. Summary and final remarks

The gradient of the parallel velocity estimated on the basis of neoclassical theory in the pedestal of ALCATOR C-Mod H-mode discharges that are close to the ELM-free to EDA transition approaches the value required for the onset of the PVS K–H instability. Moreover, the poloidal wavenumber and frequency of the QC mode that is observed in EDA, but not in ELM-free, discharges are compatible with weakly unstable PVS K–H oscillations. The hypothesis that these trigger the transition explains readily the favourable roles of high q and high triangularity and the negligible role of rational surfaces. It also accounts for the observed enhanced edge particle transport if it is assumed that the velocity gradient is frozen at its threshold value after instability onset and that the unstable layer is impermeable for neutrals (the latter hypothesis has been verified for the reference discharge). On this basis, ways of obtaining the EDA H-mode in large devices can be suggested.

Below are some concluding remarks.

(α) An effective particle diffusion coefficient can be derived from equation (11*c*), namely

$$D_{an} \cong \left(\frac{\eta_i a_{i,p}}{19\alpha L_T}\right)(\chi_{\perp,i})_{neo},$$

where $(\chi_{\perp,i})_{neo} = 3.2q^2\nu_i a_i^2$ is the neoclassical thermal conductivity. Particles thus diffuse at a rate imposed by ions rather than by electrons, as predicted in neoclassical theory (a similar conclusion was reached years ago in the context of arc experiments [17]). D_{an} and $D_{neo} = (1+q^2)\,\nu_e a_e^2$ [18] stand in the ratio

$$\frac{D_{an}}{D_{neo}} = 0.12\eta_i\left(\frac{a_{i,p}}{L_T}\right)\sqrt{\frac{m_i T_e}{m_e T_i}}\,f(Z_{eff}),$$

which yields $D_{an}/D_{neo} \approx 4$–5 for the reference discharge.

(β) Magnetic components are naturally associated with the PVS K–H instability, as observed in [19]. Electrostatic theory provides nevertheless the instability threshold quite accurately, owing to the low edge β value. Further comparison between theory and experiment can be based on the ratio of the amplitudes of the electric and magnetic fluctuations.

(γ) The theory of the PVS K–H instability has recently been extended in order to take the effect of the equilibrium temperature gradient into account [20] (the relation between magnetic and electric fluctuations has also been obtained). This extension is particularly important for a self-consistent model since $\partial_r U_{\varphi,i}$ (and, therefore, $\partial_r U_{\|,i}$) is proportional to $(\partial_r T_i)^2/T_i$ in the framework of neoclassical theory. The instability criterion remains essentially unchanged if, as in the reference discharge, $\eta_i = 1.6$ and $T_i = T_e$, except that $\alpha \cong 0.8$ (instead of $\alpha \cong 1$).

(δ) The washboard mode that has been observed on JET is, like the QC mode, not tied to a particular rational surface; it has also been interpreted as a PVS K–H oscillation [21].

(ε) It has been shown recently that flexible refuelling may provide some degree of external control of the edge plasma rotation [22, 23]. It may thus also be a tool for accessing the EDA confinement mode.

Acknowledgments

I would like to thank one of the referees for very constructive comments and my colleague M.Z. Tokař for useful discussions.

Appendix

The inertia term, $m_i[\partial_t(N_i U_{\varphi,i}) + \partial_r(N_i U_{r,i} U_{\varphi,i})]$, is the sum of two contributions: $m_i N_i(\partial_t + U_{r,i}\partial_r)\,U_{\varphi,i}$ and $m_i U_{\varphi,i}[\partial_t N_i + \partial_r(N_i U_{r,i})] = m_i \nu_{iz} N_i U_{\varphi,i}$, taking account of the continuity equation of the ions. Bringing $m_i\nu_{iz}N_iU_{\varphi,i}$ to the right-hand side of equation (3) yields the combination $-m_iN_i(\nu_{iz} + \nu_{cx})(U_{\varphi,i} - U_{\varphi,0})$. The approximation that allows us to simplify equation (3) into (4) in the steady state thus consists in replacing $-m_iN_i(\nu_{iz} + \nu_{cx})(U_{\varphi,i} - U_{\varphi,0})$ by $-m_iN_i\nu_{iz}U_{\varphi,i}$. That may modify the results quantitatively, not qualitatively: indeed $-m_iN_i(\nu_{iz} + \nu_{cx})(U_{\varphi,i} - U_{\varphi,0})$ is of the same order of magnitude and has the same sign as $-m_iN_i\nu_{iz}U_{\varphi,i}$ since the neutrals are dragged by the ions.

The assumption $\nu_{iz} \ll \nu_{cx}$, as is inherent to section 4.2, is only marginally satisfied for the present experimental conditions. Conclusions similar to those described here, in particular regarding the penetration depth, can be obtained in the limit where cold neutrals arising from the scrape off layer ($U_{\varphi,0} \ll U_{\varphi,i}$) are dominant in the neutral population.

References

[1] Rogister A.L. *et al* 2002 *Nucl. Fusion* **42** 1144
[2] Rice J.E. *et al* 2000 *Phys. Plasmas* **7** 1825
[3] D'Angelo N. 1965 *Phys. Fluids* **8** 1748
[4] Catto P.J., Rosenbluth M.N. and Liu C.S. 1973 *Phys. Fluids* **16** 1719
[5] Greenwald M. *et al* 1999 *Phys. Plasmas* **6** 1943
[6] Hutchinson I.H. *et al* 2001 *Nucl. Fusion* **41** 1391
[7] Braginskii S.I. 1965 *Reviews of Plasma Physics* vol 1 (New York: Consultants Bureau) p 205 ff
[8] Claassen H.A., Gerhauser H., Rogister A.L. and Yarim C. 2000 *Phys. Plasmas* **7** 3699
[9] Ida K. *et al* 1990 *Phys. Rev. Lett.* **74** 1995
[10] Rogister A.L. 1998 *Phys. Rev. Lett.* **81** 3663
[11] Balescu R. 1988 *Transport Processes in Plasmas* vol 2 (Amsterdam: North-Holland) p 659
[12] Mikhailovskii A.B. and Tsypin V.S. 1982 *Sov. Phys.—JETP* **56** 75
Mikhailovskii A.B. and Tsypin V.S. 1982 *Zh. Eksp. Teor. Fiz.* **83** 139
[13] Hazeltine R.D. 1974 *Phys. Fluids* **17** 961

[14] Simakov A.N. and Catto P.J. 2003 *Phys. Plasmas* **10** 398
[15] Janev R.K. *et al* 1987 *Elementary Processes in Hydrogen–Helium Plasmas* (Berlin: Springer) pp 26, 128
[16] Greenwald M. *et al* 1988 *Nucl. Fusion* **28** 2199
[17] Simon A. 1955 *Phys. Rev.* **98** 317
[18] Rutherford P.H. 1970 *Phys. Fluids* **13** 482
[19] Snipes J.A. *et al* 2001 *Plasma Phys. Control. Fusion* **43** L23
[20] Rogister A.L., Singh R. and Kaw P. 2004 *Phys. Plasmas* **11** 2106
[21] Perez C.P. *et al* 2004 *Plasma Phys. Control. Fusion* **46** 61
[22] Helander P., Fülöp T. and Catto P.J. 2003 *Phys. Plasmas* **10** 4396
[23] Singh R., Rogister A. and Kaw P. 2004 *Phys. Plasmas* **11** 129